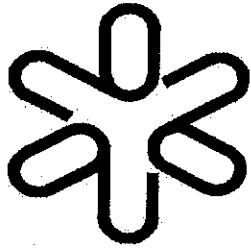# Instituto de Física
Universidade de São Paulo

Nuclear transparency and the onset of strong absorption regime in the ^{12}C + ^{24}Mg system

Lichtenthäler, R.; Lépine-Szily, A.; Hussein, M.S.

Departamento de Física Nuclear, Instituto de Física, Universidade de São Paulo, São Paulo, Brasil

"This work is dedicated to Prof. L.C. Gomes a colleague and friends"

Nuclear transparency and the onset of strong absorption regime in the $^{12}C+^{24}Mg$ system

R. Lichtenthäler, A. Lépine-Szily and M. S. Hussein

Departamento de Física Nuclear, Instituto de Física, Universidade de São Paulo

C.P.66318, 05315-970 São Paulo, SP, Brazil

June 17, 1999

Abstract

The elastic scattering of $^{12}C+^{24}Mg$ has been studied by means of a phase-shift analysis of 21 angular distributions ranging from $E_{lab} = 16$ MeV up to $E_{lab} = 40$ MeV. A tri-dimensional plot of the reflection coefficient of the S-matrix as a function of the angular momentum and the energy shows a well defined region of energy, which separates two regimes: strong absorption for higher energies and the so called "anomalous transparency regime", recently observed in this system at low energies. The Argand diagrams of the S-matrix in angular momentum space also present very contrasting behaviours in the two regions with very rapidly varying phases in the low energy region, which we associate with a parity dependent term in the S-matrix directly related to significant coupling to the elastic transfer of a ^{12}C nucleus.

An anomalous transparency has been observed[1] in the $^{12}C+^{24}Mg$ system at energies around and slightly above the Coulomb barrier ($E \leq 1.5E_b$). The angular distributions of the elastic scattering are characterized by oscillations and require a very small imaginary part in the optical potential in order to be fitted. These oscillations are present in practically the whole angular distribution, even at forward and intermediate angles, in contrast to the well-known phenomenon of Anomalous Large Angle Scattering (ALAS), which is observed at slightly higher energies ($E \geq 2.5E_b$) and is characterized by oscillating angular distributions and excitation functions at large angles[2]. The oscillations observed in the angular distributions of the systems which exhibit ALAS phenomenon can be reproduced by a background strong absorption S-matrix plus a localized perturbation normally around the grazing angular

1

momentum. This is an indication that a peripheral process is responsible for the oscillations observed at large angles. The coupling of alpha transfer channels to the elastic scattering can be the origin of this perturbation in the S-matrix[3, 4, 5, 6]. On the other hand, the anomalous transparency at low energies shows a sensitivity of the elastic scattering to the nuclear interior, whose signatures in the S-matrix are a very rapid variation of the phases and strong oscillations in the reflection coefficients, in contrast to a typical strong absorption S-matrix, which is a smooth function of the angular momentum.

In this paper we present the results of an extensive phase-shift analysis of the 21 available angular distributions of the $^{12}C +^{24} Mg$ elastic scattering[4, 6, 7, 8] which show the clear transition that occurs between the two regimes. The phase-shift analysis was performed using a method we recently developed [9], which allows the determination of the elastic S-matrix elements and their associated errors, using a chi-square minimization algorithm specially developed for the scattering problem. The method has proven to be quite versatile at low energies, where the convergence is achieved very rapidly.

There are two important aspects in the phase-shift analysis: the starting S-matrix for the search and the maximum number of partial waves used in the search ($lmax$). As a starting point for the analysis, we used the S-matrix generated by the optical model potential named X3 in ref. [4]. This potential reproduces well the forward angle region and the mean slope of the angular distributions in the range of energy studied, but not the oscillations.

For $l \geq lmax$ we use the S-matrix elements calculated by the X3 optical potential. For $l < lmax$ the S-matrix elements are obtained by search. The maximum angular momentum in the analysis was choosen by the condition $|S_{lmax}| \geq .93$. This analysis is more reliable, as far as ambiguities are concerned due to the fact that the errors of the S-elements are also calculated. We observed that when the error bars are small, the final S-matrix is practically independent of the starting point of the search and of the maximum number of partial waves used in the analysis. On the other hand, if the error bars are big a large ambiguity in the final S-matrix is observed. The precision of the final S-matrices is related to the quality and completeness of the experimental angular distributions.

The result of this analysis is presented in figure 1 in a tri-dimensional plot of the reflection coefficients ($|S_l(E)|$) as a function of the laboratory energy and of the angular momentum. We can observe the clear transition between the two regimes occuring at laboratory energies around 28 MeV. The Coulomb barrier for this system is $E_{lab} = 18.5$ MeV, calculated using the best fit optical potential of reference [1]. The reflection coefficients for energies above 28MeV show a relatively smooth transition from unity, at high angular momentum values, to very low values at low partial waves. This is a typical strong absorption behaviour with a well defined value of the grazing

2

angular momentum. The very small perturbations observed in this S-matrix at low l-values are responsible for the ALAS phenomenon. Below 28MeV the situation is completely different, with strongly oscillating reflection coefficients as a function of the energy and angular momentum. In this situation, the grazing trajectories are not well defined in the sense that many different values of angular momentum can be assigned to the condition $|\dot{S}_l| = 0.5$.

In figures 2a,b,c,d we plot the reflections coefficients(left) and Argand diagrams(right) $(S_r X S_i)$ of the S-matrices as a function of the angular momentum at four laboratory energies: 40, 31.2, 23 and 20MeV. At the two higher energies we observe a typical strong absorption behaviour either in the reflection coefficients or in the Argand diagrams which start at $S = 1$ for high angular momenta and go smoothly to zero for low angular momenta. The Argand diagram is restricted to the first quarter of the complex plane $S_R \geq 0$ and $S_I \geq 0$ showing a small positive nuclear phase corresponding to an attractive nuclear potential. At lower energies, on the other hand, one can observe loops in the Argand diagrams showing a rapidly increasing real phase for decreasing angular momenta. The presence of these loops traversed in the anti-clockwise sense, as l decreases, can be due to a parity dependent term in the S-matrix, as we show qualitatively below.

In fig.2e we plot the S-matrix obtained by the simple parametrization:

$$S = S_0 + (-1)^l S_{et} \tag{1}$$

where S_0 is a background S-matrix taken to be of the Ericsson form:

$$S_0 = \frac{1}{1 + exp(\frac{(lg_0-l)}{\Delta_0} - i\alpha_0)} \tag{2}$$

and S_{et} is a parity dependent term given by:

$$S_{et} = A\frac{exp(\frac{lg-l}{\Delta} - i\alpha)}{(1 + exp(\frac{lg-l}{\Delta} - i\alpha))^2} \tag{3}$$

The values of the parameters are given:$lg_0 = 7$, $\Delta_0 = 1.0$, $\alpha_0 = 0.7$ $lg = 4$, $\Delta = 1.0$, $\alpha = -0.7$, and $A = 2.5$. The loops in the corresponding Argand diagrams in fig. 2e(right), are introduced by the term S_{et}. In order to have the correct sense, loop traversed in anti-clockwise sense as l decreases, it is necessary to use a negative nuclear phase parameter α. If α is positive, the sense of traversing the loops is opposite to the observed in the experimental Argand diagrams. As a negative nuclear phase corresponds to a repulsive nuclear potential, we conclude that the interaction responsible for the parity dependence is repulsive. This is in agreement with the analysis presented in ref. [10] where we found a positive form factor.

3

The elastic transfer of a ^{12}C between the ^{24}Mg target and the ^{12}C projectile can be the physical origin of this parity dependence in the S-matrix as suggested in [10].

Another possible explanation for the loops observed in the Argand diagrams in l-space is the presence of Regge poles, which would come closer to the real axis in the low energy region, where transparency comes in. The presence of Regge poles would be an indication of a resonant regime at these energies, probably due to quasi-molecular states in the ^{36}Ar composite system. In order to test this hypothesis, we plotted Argand diagrams of the S-matrices as a function of energy for fixed angular momentum. The Argand diagrams in the complex energy plane show an apparently chaotic behaviour and no loops were observed for any angular momentum involved in the scattering. This indicates that the resonances, if present, must have widths smaller than 330 KeV(C.M.) which is the energy step of the measurements at low energies. For this reason we discard the hypothesis of molecular resonances of widths greater than 330 KeV.

An interesting phenomenon observed in our analysis, is the sudden onset of strong absorption at energies ≈ 8 MeV(c.m) above the Coulomb barrier. This could be associated with a threshold effect related to the opening of the $3 - \alpha$ cluster (Hoyle) resonance channel in ^{12}C.

Recently we have presented evidence, based on optical model analysis, in support of strong coupling of the elastic $^{12}C+^{24}Mg$ channel to the elastic transfer channel $^{24}Mg+^{12}C$ near barrier energies which strongly influences the angular distributions. Further evidence in support of a strong two ^{12}C clustering effect in the ground state of ^{24}Mg is presented here. This finding has important implications on the two ^{12}C cluster nature of the ground state of ^{24}Mg and may potentially be significant in nuclear astrophysics.

Acknowledgements

References

[1] A. Lépine–Szily, W. Sciani, Y. K. Watari, W. Mittig, R. Lichtenthäler, M. M. Obuti, J. M. Oliveira Jr., A. C. C. Villari, Phys. Lett. **B 304**, (1993) 45.

[2] P. Braun-Munzinger and J. Barrete, Phys. Reports **vol.87** (1982)

[3] R. Lichtenthäler, A. Lépine-Szily, A.C.C. Villari,W. Mittig, V.J.G. Porto,C.V. Acquadro, Phys. Rev. **C26**, 2487, (1982)

[4] R. Lichtenthäler, A. Lépine-Szily, A.C.C. Villari, O. Portezan Filho, Phys. Rev. **C39**, 884, (1989)

[5] A. Lépine-Szily, R. Lichtenthäler, M.M. Obuti, J. Martins de oliveira Jr., O. Portezan Filho, W. Sciani, A.C.C. Villari Phys. Rev.**C40**, 681, (1989)

[6] A. Lépine-Szily, M. M. Obuti, R. Lichtenthäler,J. M. Oliveira Jr., A.C.C. Villari, Phys. Lett **B 243** (1990) 23.

[7] W. Sciani, A. Lépine–Szily, R. Lichtenthäler, P. Fachini, L.C. Gomes, G. F. Lima, M. M. Obuti, J. M. Oliveira Jr., A. C. C. Villari, Nucl. Phys. **A 620** (1997) 91.

[8] M.C. Mermaz, A. Greiner, B.T. Kim, M.J. LeVine, E. Müller, M. Ruscev, M. Petrascu, M. Petrovici, V. Simion, Phys. Rev. **C24**,1512, (1981)

[9] V. Chisté, R. Lichtenthäler, A.C.C. Villari, L.C. Gomes Phys. Rev. **C54**, 784, (1996)

[10] A. Lépine-Szily, M.S. Hussein, R. Lichtenthäler, J. Cseh and G. Lévai Phys. Rev. Lett. **C82** (1999)3972

1 Figure Captions

Figure 1. Plot of the reflection coefficients as a function of the laboratory energy and angular momentum.

Figure 2(left) The reflection coefficients for 20MeV(a), 23MeV(b), 31.2MeV(c), 40MeV(d) and for the S-matrix of equation 1(e). The dashed line in fig2(e) is the background reflection coefficients ($|S_0|$, eq.1). See text for details.

Figure 2(right) Argand diagrams of the S-matrix as a function of the angular momentum for the same energies and for the S-matrix of equation 1. See text for details.